



Temporal Clusters of Kawasaki Disease Cases Share Distinct Phenotypes That Suggest Response to Diverse Triggers

Jane C. Burns, MD^{1,2}, Laurel L. DeHaan, MS³, Chisato Shimizu, MD¹, Emelia V. Bainto, BA¹, Adriana H. Tremoulet, MD, MAS^{1,2}, Daniel R. Cayan, PhD³, and Jennifer A. Burney, PhD⁴

Objective To test the hypothesis that cases of Kawasaki disease within a temporal cluster have a similar pattern of host response that is distinct from cases of Kawasaki disease in different observed clusters and randomly constructed clusters.

Study design We designed a case-control study to analyze 47 clusters derived from 1332 patients with Kawasaki disease over a 17-year period (2002-2019) from a single clinical site and compared the cluster characteristics with those of 2 control groups of synthetic Kawasaki disease clusters. We defined a “true” Kawasaki disease cluster as at least 5 patients within a 7-day moving window. The observed and synthetic Kawasaki disease clusters were compared with respect to demographic and clinical characteristics and median values for standard laboratory data using univariate analysis and a multivariate, rotated empirical orthogonal function analysis.

Results In a univariate analysis, the median values for age, coronary artery z-score, white blood cell count, erythrocyte sedimentation rate, C-reactive protein, and age-adjusted hemoglobin for several of the true Kawasaki disease clusters exceeded the 95th percentile for the 2 synthetic clusters. REOF analyses revealed distinct patterns of demographic and clinical measures within clusters.

Conclusions Cases of Kawasaki disease within a cluster were more similar with respect to demographic and clinical features and levels of inflammation than would be expected by chance. These observations suggest that different triggers and/or different intensities of exposures result in clusters of cases of Kawasaki disease that share a similar response pattern. Analyzing cases within clusters or cases who share demographic and clinical features may lead to new insights into the etiology of Kawasaki disease. (*J Pediatr* 2021;229:48-53).

Kawasaki disease, a pediatric self-limited vasculitis that affects the coronary arteries, has eluded attempts to discover its etiology for more than 4 decades.¹ Epidemiologic clues have provided valuable insight into the nature of the disease, including the genetic predisposition that underlies susceptibility.² The elucidation of the distinct seasonality, the lack of documented person-to-person spread, and the spatiotemporal clustering of cases all suggest a fluctuating exposure that triggers the disease.³ Clinical features of the illness, including mucosal inflammation of the lips, tongue, and upper airway coupled with cervical lymphadenopathy and hoarseness, point to a trigger that enters through the nasopharynx.^{4,5} Specific atmospheric patterns have been linked to clusters of cases of Kawasaki disease that may increase exposure to the causative trigger.³

Although Kawasaki disease is conceptualized as a monomorphic disease, it may be more accurate to characterize it as a syndrome with subtle variations among clinical subgroups. Certain clinical features are not universal among patients with Kawasaki disease; these include the “node-first” presentation with fever and cervical lymphadenopathy, the specific injury pattern to the tongue usually associated with bacterial toxins (strawberry tongue), and the characteristic periungual desquamation in the convalescent phase.^{5,6} The prospective collection of detailed demographic and clinical data for cases of Kawasaki disease treated at Rady Children’s Hospital San Diego (RCHSD) allowed statistical analysis of the temporal pattern of cases of Kawasaki disease over many years, which revealed a clustering of cases beyond what would be expected due to Kawasaki disease seasonality and trends alone. Demographic and clinical characteristics of cases within these temporal clusters were compared with those of synthetic control clusters derived from either reshuffling members of clusters or creating clusters of same-season cases that did not occur within observed clusters. The results highlight the shared features within a cluster

CA	Coronary artery
CRP	C-reactive protein
ESR	Erythrocyte sedimentation rate
RCHSD	Rady Children’s Hospital San Diego
REOF	Rotated empirical orthogonal function
WBC	White blood cell count
Zhemo	Hemoglobin concentration normalized for age
Zworst	Maximal CA z-score for the right CA and left anterior descending artery as determined by echocardiography

From the ¹Department of Pediatrics, University of California San Diego, La Jolla, CA; ²Rady Children’s Hospital San Diego, San Diego, CA; and ³Scripps Institution of Oceanography and ⁴School of Global Policy and Strategy, University of California San Diego, La Jolla, CA

The authors declare no conflicts of interest.

0022-3476/\$ - see front matter. © 2020 Elsevier Inc. All rights reserved.
<https://doi.org/10.1016/j.jpeds.2020.09.043>

and suggest that future research on etiology should prioritize the separate analysis of cases that share similar subphenotypes.

Methods

Study Population

We enrolled 1332 patients with Kawasaki disease who met American Heart Association guidelines for complete or incomplete Kawasaki disease and were diagnosed and treated at RCHSD between January 1, 2002, and March 31, 2019.⁷ The worst coronary artery (CA) z-score was defined as described previously.⁸ The collection of data was approved by the Institutional Review Board at the University of California San Diego, and parents and participants gave signed informed consent or assent as appropriate.

Identification of Temporal Clusters

We computed the distribution density of case onsets (cases per 7-day period) across the entire sample. We took the value associated with the high tail of the 95% CI (97.5th percentile) of the density distribution as the starting definition for a temporal cluster, which was 5 or more cases in 7 days (**Figure 1**). Across the time series, any day that was part of a moving window in which case density equaled or exceeded 5 cases in 7 days was classified as a cluster day (irrespective of whether or not it had a case onset), and any Kawasaki disease onset falling in that window was classified as a “cluster” case. Cases outside of that window were classified as “noncluster” cases of Kawasaki disease.

Calculation of Cluster-Level Characteristics

We used a set of 14 clinical and demographic quantities to calculate cluster-level characteristics:

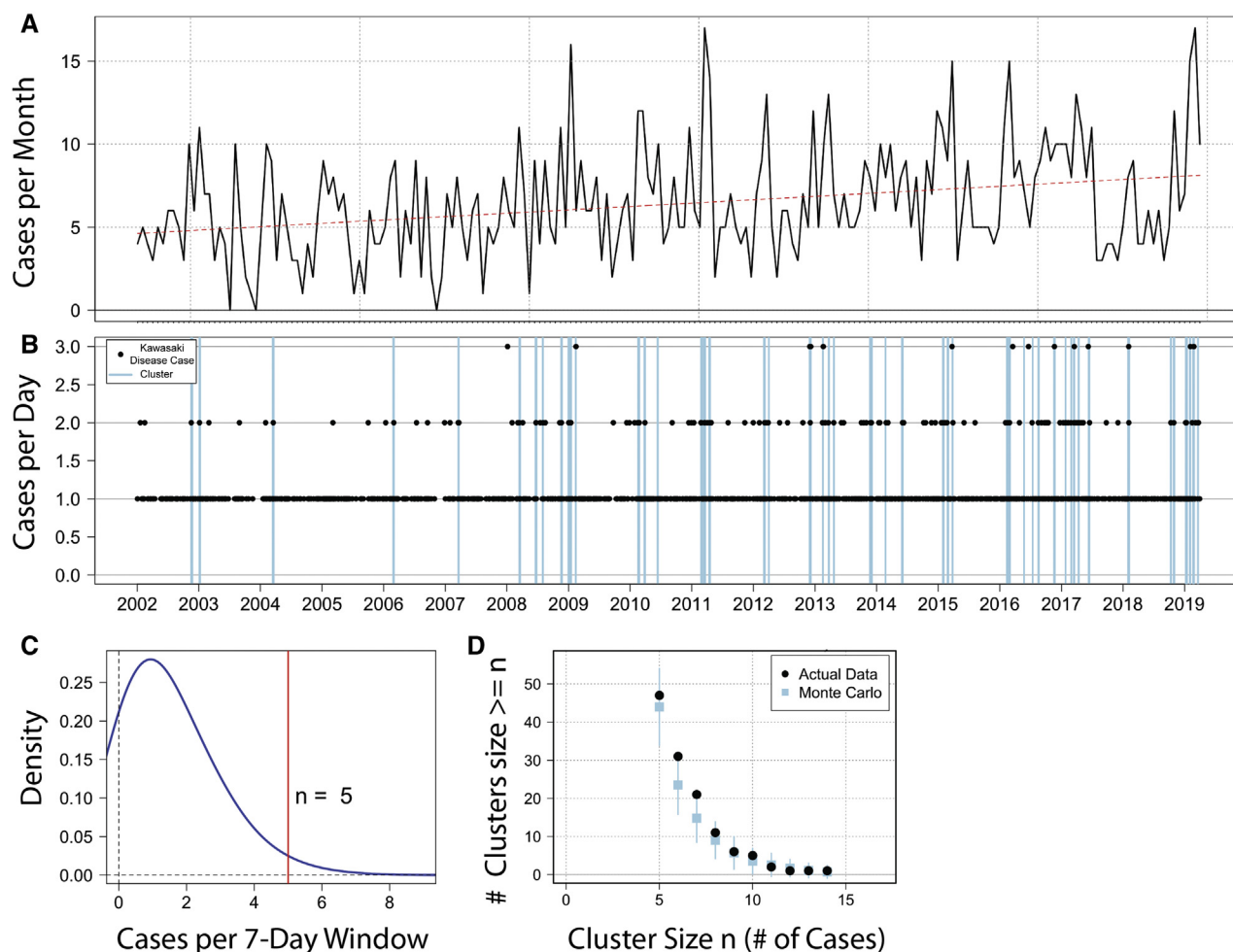


Figure 1. Study area and temporal clustering. **A**, Monthly distribution of 1332 cases and temporal trend in cases of Kawasaki disease seen at RCHSD between January 2002 and March 2019. **B**, Time series of daily cases (black dots) and clusters (blue lines), defined as 5 or more cases in 7 days. **C**, Distribution of case density for the study period; $n = 5$ is the 97.5th percentile density. **D**, Monte Carlo simulation drawing 100 time series of 1332 randomly selected dates with the same time trend and seasonality as the true data (blue squares). Comparing that with the true data (black dots) shows more clusters of 6 or 7 cases in the true data than would be expected from a random distribution of established trends and seasonality.

- Patient residence longitude and latitude. Owing to the very large geographic catchment area, we used geospatial coordinates to understand potential spatial dependence of clinical clusters. For cluster-level summaries, we used median longitude and latitude. Because of the uneven distribution of ethnic/racial groups in our region, we considered these geospatial coordinates as a surrogate for race/ethnicity.
- Patient age at date of onset, with the first day of fever designated as illness day 1. For cluster-level summaries, we used median age at onset.
- Laboratory data before intravenous immunoglobulin infusion and within the first 15 days after fever onset: White blood cell count (WBC), platelet count, erythrocyte sedimentation rate (ESR), C-reactive protein (CRP), and hemoglobin concentration normalized for age (Zhemo). Maximal CA z-scores for the right CA and left anterior descending artery (Zworst) were determined by echocardiography. For cluster-level analysis, we used median values for each of these quantities. Hepatic enzyme elevations were analyzed as a dichotomous variable (alt_abnormal), with a normal value defined as below the age-adjusted upper limit of normal for alanine amino transferase (<60 IU) and an abnormal value defined as >100 IU. For cluster-level analysis, mean values were used.
- Patient sex and the presence of a strawberry tongue, enlarged cervical lymph nodes (>1.5 cm), and convalescent peeling fingers or toes. For cluster-level summaries of these characteristics, we used mean values.

We also computed the variance of each attribute for each cluster as a metric of similarity of patients within a cluster. For any clusters that included patients who presented beyond illness day 15, we calculated cluster-level values excluding these cases, to prevent skewing of the data from patients diagnosed later in the illness when laboratory values of inflammation might be normalizing. Overall, there were 18 cases whose laboratory data were excluded from analysis because of diagnosis beyond day 15.

Generation of Synthetic Clusters for Comparison. We created 100 sets of synthetic clusters of the same size distribution as the observed clusters, hereinafter termed true clusters; we created synthetic clusters by shuffling cluster membership among the 315 cluster cases of Kawasaki disease (ie, shuffled clusters). The universe of cluster cases was randomly reallocated to 47 groups of the same size as the true observed temporal clusters. We also created a set of synthetic clusters drawn from non-Kawasaki disease cluster cases that occurred in any year but within the same season (ie, control clusters) ([Appendix](#); available at www.jpeds.com).

Univariate Analysis: Statistical Analysis of True Clusters Compared with Synthetic Clusters. We assessed the degree to which each individual cluster was anomalous relative to both sets of synthetic clusters by testing whether the cluster-average value for each clinical characteristic lay outside the range of averages among the comparison groups;

for example, we compared the median age of true cluster 7 to the distribution of median age in 100 shuffled cluster 7s and 100 control cluster 7s. We calculated a *P* value for each true cluster compared with these groups. We also compared the variances of attributes in the true clusters compared with the synthetic comparison clusters; for example, we compared the variance in age of true cluster 7 with the variance in age in 100 shuffled cluster 7s and 100 control cluster 7s.

We also compared the full distribution of average values and variances in the true clusters with a sample drawn from each of the comparison groups. This allowed us to assess whether the true clusters as a whole represented a departure from the comparison groups; that is, does the temporal clustering overall produce a different distribution of traits beyond individual clusters? We took a random draw of 1 of each of the 47 groups of 100 shuffled clusters and 1 of each of the 47 groups of 100 control clusters and compared, for example, the distribution of 47 true cluster median ages with the distributions of these 2 groups of 47 synthetic clusters.

Multivariable Analysis: Rotated Empirical Orthogonal Function Analysis. A key question is whether existing sets of clusters differ repeatedly from other clusters by combinations of clinical or demographic characteristics either in addition to or in lieu of individual characteristics. To assess this, we conducted a rotated empirical orthogonal function (REOF) analysis.⁹ This is similar to principal component analysis, extracting statistically independent “modes” of Kawasaki disease, wherein the first few explain a relatively large portion of the variance of the entire data sample. Varimax rotation was used to identify patterns of unusually high or low expression in the demographic or clinical characteristics in subsets of the clusters. Details of REOF generation are provided in the [Appendix](#).

Results

Kawasaki Disease Clusters

The dataset comprised 47 clusters consisting of 315 cases of Kawasaki disease ([Figure 1](#)). To determine whether more cases of Kawasaki disease had their onset in clusters than would be expected at random, we used a Monte Carlo analysis to create 100 time series with an equivalent number of cases from all days in the study period, which would account for seasonality and diagnosis trends over time. We tallied the clusters in these timeseries according to the same cluster definition and calculated the distribution of clusters. Although a certain number of clusters of 5 or more cases in 7 days occurred at random, a larger number of clusters of 6–7 cases in 7 days occurred in the true data compared with the Monte Carlo simulation ([Figure 1, E](#)). This indicated that more cases of Kawasaki disease were included in clusters than would be expected by chance. However, grouped together, the demographic and clinical characteristics of the 315 cluster cases of Kawasaki disease were compared with the 1017 noncluster cases of Kawasaki disease, and no significant differences were noted ([Table](#)).

In the univariate analysis, cluster-level averages of demographic and clinical characteristics were compared between the set of 47 true Kawasaki disease clusters and 100 sets of 47 synthetic clusters of equal size created either by randomly shuffling membership of cluster cases (referred to as shuffled clusters) or by randomly creating clusters from noncluster cases of Kawasaki disease within the same season as the true cluster (referred to as control clusters) (Figure 2; available at www.jpeds.com). Striking differences were noted between individual true clusters and synthetic clusters for the following variables: age, ESR, and the presence of enlarged lymph nodes or strawberry tongue. For all the characteristics, the difference in the true cluster distribution vs either set of synthetic clusters was highly significant (Appendix, Figure 1).

We next analyzed the coherence of characteristics of cases within true clusters. We calculated the intraclass correlation coefficient, which shows the percentage of the variance occurring between vs within clusters (Appendix, Table). In this analysis, lymph node, WBC, ESR, age, and platelet count were significantly more similar within true clusters than between true clusters ($P = .007, .008, .009, .035$, and $.045$, respectively). To help visualize the variation within and between clusters, individual cluster distributions for the true clusters are shown for several characteristics in Appendix, Figure 2.

Interpretation of REOFs. In the multivariable analysis, the first 4 REOFs together explained 55% of the total variance of the true clusters: REOF1 explained 18%, REOF2 explained

13%, and REOF3 and REOF4 each explained 12%. For each of these 4 REOFs, the highest weightings on the 14 characteristics were identified to determine the defining characteristics presented in the true clusters (Figure 3, A). Several of the defining characteristics in the multivariable analysis also were identified as strongly expressed features in the univariate analysis. For REOF1, the defining characteristics (the characteristics with a weight larger than one SD) were ESR, CRP, and Zhemo. Clusters that loaded strongly (positively or negatively) onto this REOF had a higher than average ESR and CRP and a lower than average Zhemo or had a lower than average ESR and CRP and a higher than average Zhemo (Appendix, Figure 3).

The prevalence of these defining characteristics can be seen in Figure 3, B, evaluating this pattern from REOFs obtained in a Monte Carlo sampling of the true clusters vs those from the shuffled and control clusters. From the true set of Monte Carlo samples, an REOF was found with the defining characteristics ESR, CRP, and Zhemo almost 50% of the time, whereas from the shuffled clusters, this relationship occurred <25% of the time, and from the control clusters it occurred <15% of the time. This indicates that the true clusters expressed a much stronger relationship among these 3 characteristics than would be expected by chance.

The defining characteristics of REOF2 were age, sex, and WBC, with age and fraction male presenting in the same direction and WBC in the opposite direction. Thus, some clusters had older patients with a higher percentage of males and lower WBC, whereas other clusters had younger patients with a lower percentage of males and higher WBC. Because

Table. Demographic and clinical laboratory characteristics of patients with Kawasaki disease within the 47 clusters (cluster Kawasaki disease) and not in clusters (noncluster Kawasaki disease)

Characteristics	Cluster Kawasaki disease (N = 315)	Noncluster Kawasaki disease (N = 1017)	P value
Age at onset, y, median (IQR)	2.8 (1.5-5.2)	2.7 (1.4-4.8)	NS
Male sex, n (%)	197 (63)	626 (62)	NS
Ethnicity, n (%)			NS
Asian	44 (14)	156 (15)	
Black	11 (3)	40 (4)	
White	77 (24)	238 (23)	
Hispanic	115 (37)	350 (34)	
More than one race	61 (19)	202 (20)	
Others or unknown	7 (3)	31 (4)	
Clinical signs, n/N (%) ^a			
Strawberry tongue	120/105 (53.3)	357/223 (61.6)	NS
Lymph node enlargement	102/211 (32.6)	329/1010 (32.6)	NS
Peeling	175/140 (55.6)	618/398 (60.8)	NS
CA Zworst score, median (IQR)	1.6 (1.1-2.5)	1.7 (1.1-2.5)	NS
Illness day of lab data, median (IQR)	5 (4-7)	6 (4-7)	
Laboratory data, median (IQR)			
WBC, $\times 10^3/\mu\text{L}$	13.6 (10.5-17.5)	13.1 (10.4-17.1)	NS
Zhemo	-1.3 (-2.2 to -0.3)	-1.3 (-2.1 to -0.4)	NS
Platelets, $\times 10^3/\mu\text{L}$	355 (280-441)	365 (284-461)	NS
ALT, IU/L	43 (24-109)	43 (24-114)	NS
ESR, mm/h	59 (37-78)	60 (41-75)	NS
CRP, mg/dL	6.3 (3.8-16.2)	6.9 (4.1-15.2)	NS
Latitude	32.91 (32.74-33.14)	32.91 (32.74-33.15)	NS
Longitude	-117.09 (-117.18 to -117.03)	-117.10 (-117.20 to -117.04)	NS

NS, not significant; ALT, alanine aminotransferase.

CA Zworst is defined as the largest internal CA diameter during the first 6 weeks after fever onset for the right and left anterior descending CAs normalized for body surface area and expressed as SD units from the mean. Latitude and longitude refer to the subject's primary residence.

^aN subjects with the finding/n subjects for whom the observation of the presence or absence of the finding was made.

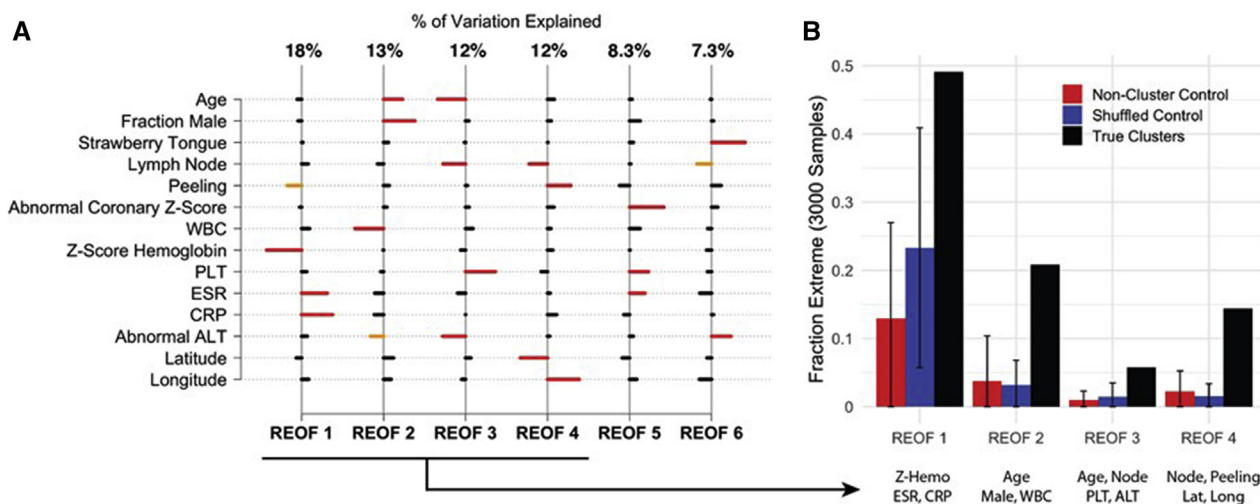


Figure 3. REOFs. **A**, The first 4 REOF modes, with their respective fraction of variance (% of total), showing combinations of patient demographic and clinical characteristics that were prevalent in the 47 Kawasaki disease clusters. Horizontal bars indicate, for a given REOF, the characteristics that associated positively (to the right) or negatively (to the left). Red bars designate characteristics for a given REOF that associate most strongly, with weights >1.1 SD. Orange bars indicate moderately strong associations, with weights between 0.9 and 1.1 SD. **B**, From the Monte Carlo trials, the fraction of REOFs from control clusters, shuffled clusters, and true clusters that exhibit the defining characteristics of the leading 4 REOFs from the true clusters shown in **A**.

REOF2 captured less variability in the overall cluster universe than REOF1, these defining characteristics were less prevalent than the REOF1 defining characteristics, but still occurred $>20\%$ of the time in the true cluster population. As with REOF1, this relationship was much stronger in the true clusters than in the synthetic clusters; both shuffled clusters and control clusters produced this combination in only approximately 3% of the 3000 Monte Carlo trials.

REOF3 described the relationships among age, lymph nodes, and alt_abnormal in one direction and platelet count in the other direction. REOF4 described relationships among lymph nodes, periungual peeling, and location of patient residence; positive latitude with negative longitude indicated clusters from the northwest portion of the catchment area. Although these REOFs were less prevalent than REOF1 and REOF2, the Monte Carlo trials yielded such patterns significantly more frequently in the true clusters than in either the control or shuffled clusters.

Discussion

Historically, Kawasaki disease has been considered a monomorphic disease, with research efforts focused on these patients as a homogenous group. However, our clinical experience in diagnosing and treating patients with Kawasaki disease has suggested that many of the classic features of Kawasaki disease are not universal, and that patients with certain subphenotypes are not evenly distributed over time, even after accounting for seasonality. Our analysis focused on temporal Kawasaki disease clusters and examined the characteristics of cases within and across clusters, as well as noncluster cases, in the RCHSD time series.

A series of tests indicated that individual clusters exhibited distinctive clinical and demographic characteristics. First, temporal clusters occurred more often than would be expected by chance. Second, in assessing whether cases of Kawasaki disease within these true clusters differed from cases of Kawasaki disease not in clusters, we found that the overall central tendencies were similar in cluster and noncluster cases (Table). Thus, it was not simply a question of clustered cases being different than nonclustered cases. Third, the data revealed important differences between characteristics of individual clusters, and the distribution of characteristics differed significantly between the true clusters and the 2 sets of synthetic control clusters (Figure 3).

The finding that cases of Kawasaki disease within a cluster were more similar with respect to demographic and clinical features and levels of inflammation than would be expected by chance has important implications for research. The data suggest that either different triggers or different intensity of exposures result in clusters of cases of Kawasaki disease that share a similar response pattern, likely influenced by host genetics. This observation resonates with the current observations of the immune response to the severe acute respiratory syndrome coronavirus 2 virus creating the multi-system inflammatory syndrome in children, which shares many clinical features with Kawasaki disease.¹⁰

In the univariate analysis, ESR and CRP, both markers of systemic inflammation, were markedly elevated in certain clusters but not others. In the multivariable REOF analysis, it was further revealed that these measures of inflammation when elevated were more likely to be associated with low hemoglobin levels and vice versa (lower measures of inflammation associated with normal hemoglobin). Although this

makes sense biologically, the important finding was that some clusters had this composite feature, whereas other clusters did not.

With respect to clinical features, cases manifesting strawberry tongue or lymph node-first presentation also clustered, as did cases without these clinical features (**Figure 2**). Strawberry tongue is a specific mucosal injury pattern that involves the sloughing of the cornified tips of the filiform papillae and is associated with bacterial toxin-mediated disease.¹¹ Overall in our time series, only 477 of 805 patients (59.3%) had this phenotype at the time of diagnosis, but strawberry tongue registered quite strongly as one of the important characteristics in true clusters, in which its distribution differed from that in synthetic clusters (**Appendix, Figure 1, M**). The lymph node first presentation suggests an exaggerated immune response in regional lymph nodes to an antigenic stimulus that enters through the mucosal surfaces of the posterior oropharynx. Children presenting with only fever and enlarged cervical lymph nodes during the first week of illness have been described and represented 32.6% of patients from our center.⁵ The clustered presence or absence of these phenotypes in patients with Kawasaki disease differed significantly from the 2 groups of synthetic clusters, possibly suggesting that the patients with Kawasaki disease within these clusters were responding to different stimuli leading to these different clinical presentations. Similarly, laboratory evidence of inflammation was either high or low in different clusters, again suggesting a nonrandom distribution of these features.

In the REOF analysis, certain laboratory and clinical features were associated within the true clusters more often than expected by chance. Some of these statistical findings were consistent with our understanding of the biology of Kawasaki disease. For example, higher levels of inflammatory markers ESR and CRP were linked to more pronounced anemia and vice versa. Similarly, in REOF5, higher Zmax was linked to higher ESR and platelet count. However, other relationships, such as REOF3, which describes relationships among older age, enlarged lymph nodes, and elevated liver enzymes with lower platelet count were unexpected. Thus, new relationships of features revealed by the analysis could be used to group patients for studies of genetic susceptibility and molecular investigations of potential etiologic agents.

These observations suggest that different triggers or differing intensities of exposure may operate to produce cases of Kawasaki disease that cluster temporally and share a similar response pattern. Important insight into the different etiologies of Kawasaki disease may be gained by focusing on patients who share the demographic and clinical phenotypes identified in these analyses. ■

This work supported in part by a grant to JCB from the Gordon and Marilyn Macklin Foundation.

Submitted for publication Jul 10, 2020; last revision received Sep 1, 2020; accepted Sep 18, 2020.

Reprint requests: Jane C. Burns, MD, 9500 Gilman Dr, La Jolla, CA 92093-0641. E-mail: jcburns@health.ucsd.edu

References

1. Kawasaki T, Kosaki F, Okawa S, Shigematsu I, Yanagawa H. A new infantile acute febrile mucocutaneous lymph node syndrome (MLNS) prevailing in Japan. *Pediatrics* 1974;54:271-6.
2. Onouchi Y. The genetics of Kawasaki disease. *Int J Rheum Dis* 2018;21:26-30.
3. Rypdal M, Rypdal V, Burney JA, Cayan D, Bainto E, Skochko S, et al. Clustering and climate associations of Kawasaki disease in San Diego County suggest environmental triggers. *Sci Rep* 2018;8:16140.
4. Leuin SC, Shanbhag S, Lago D, Sato Y, Sun X, Jain S, et al. Hoarseness as a presenting sign in children with Kawasaki disease. *Pediatr Infect Dis J* 2013;32:1392-4.
5. Kanegaye JT, Van Cott E, Tremoulet AH, Salgado A, Shimizu C, Kruk P, et al. Lymph node-first presentation of Kawasaki disease compared with bacterial cervical adenitis and typical Kawasaki disease. *J Pediatr* 2013;162:1259-63. 1263.e1-2.
6. Wang S, Best BM, Burns JC. Periungual desquamation in patients with Kawasaki disease. *Pediatr Infect Dis J* 2009;28:538-9.
7. McCrindle BW, Rowley AH, Newburger JW, Burns JC, Bolger AF, Gewitz M, et al. Diagnosis, treatment, and long-term management of Kawasaki disease: a scientific statement for health professionals from the American Heart Association. *Circulation* 2017;135:e927-99.
8. Skochko SM, Jain S, Sun X, Sivilay N, Kanegaye JT, Panchari J, et al. Kawasaki disease outcomes and response to therapy in a multiethnic community: a 10-year experience. *J Pediatr* 2018;203:408-15.e3.
9. Richman MB. Rotation of principal components. *Int J Climatol* 1986;6:293-335.
10. Whittaker E, Bamford A, Kenny J, Kafrou M, Jones CE, Shah P, et al. Clinical characteristics of 58 children with a pediatric inflammatory multisystem syndrome temporally associated with SARS-CoV-2. *JAMA* 2020;324:259-69.
11. Kole A, Chandakole D. Images in clinical medicine. Strawberry tongue. *N Engl J Med* 2015;373:467.

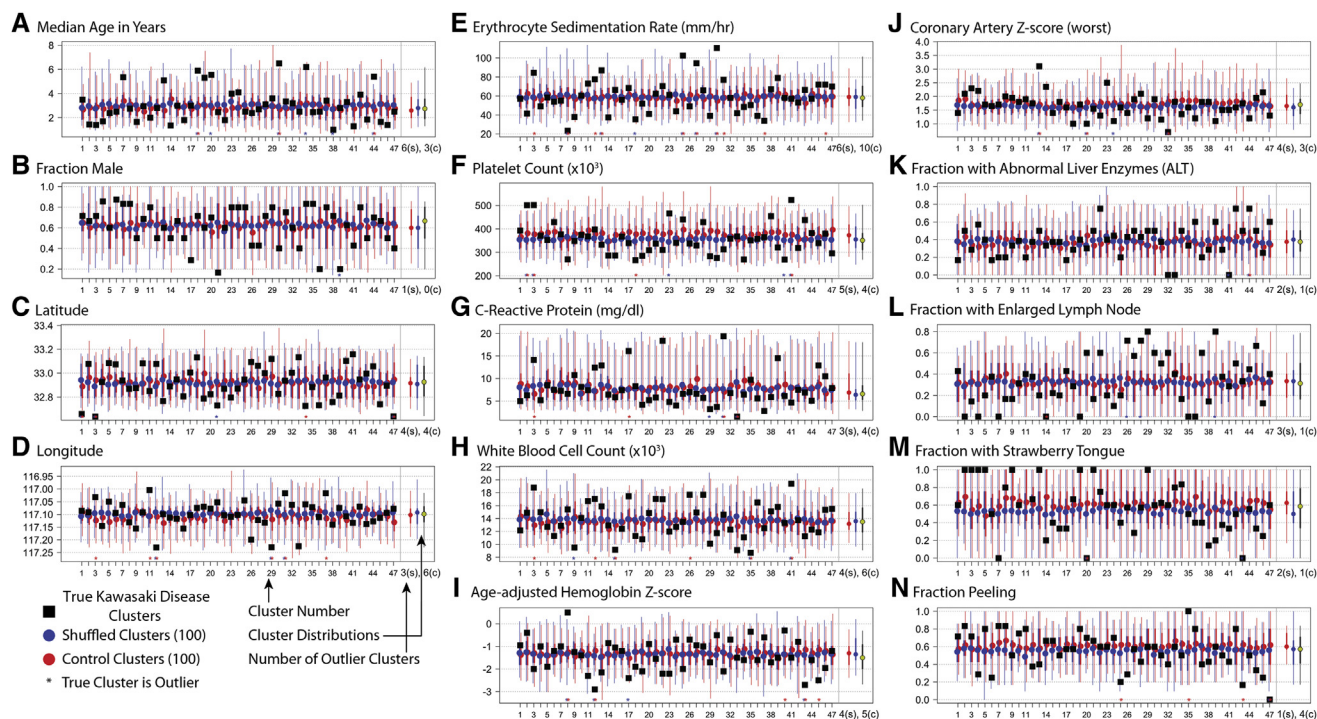


Figure 2. Cluster-level averages of patient demographic and clinical characteristics (A-N). Observed cluster-level averages for 47 Kawasaki disease clusters (*black squares*) compared with 100 equal-size synthetic clusters created by (*blue*) randomly shuffling cluster membership of cluster cases of Kawasaki disease (*shuffled clusters*), and (*red*) randomly drawn noncluster cases of Kawasaki disease from the same season as the true cluster (*control clusters*). For both comparison groups, the dots show the mean value of 100 iterations, thick lines show the IQR (25th–75th percentiles), and thin lines show the inner 95th percentile of the distribution. Red and blue asterisks at the base of each figure indicate whether the true value for the given cluster lies outside the 95th percentile of either comparison distribution; these are totaled at the lower right of the figure to provide a summary of how many of the true clusters are extreme compared with the 2 comparison groups. s, shuffled; c, control. At the right of the individual clusters, the summary of both comparison sets and the true data (*yellow circle*) are presented.